The Egorov property in perturbed cat maps

2007 J. Phys. A: Math. Theor. 40 9771

(http://iopscience.iop.org/1751-8121/40/32/004)

IOP Publishing Journal of Physics A: Mathematical and Theoretical

J. Phys. A: Math. Theor. **40** (2007) 9771–9781 doi:10.1088/1751-8113/40/32/004

The Egorov property in perturbed cat maps

Martin Horvat[1,2] **and Mirko Degli Esposti**[2]

[1] Physics Department, Faculty of Mathematics and Physics, University of Ljubljana, Slovenia
[2] Department of Mathematics, University of Bologna, Italy

E-mail: martin.horvat@fmf.uni-lj.si and desposti@dm.unibo.it

Received 19 April 2007, in final form 25 June 2007
Published 24 July 2007
Online at stacks.iop.org/JPhysA/40/9771

Abstract
We study the time evolution of the quantum-classical correspondence (QCC) for the well-known model of quantized perturbed cat maps on the torus in the very specific regime of semi-classically small perturbations. The quality of the QCC is measured by the overlap of the classical phase-space density and corresponding Wigner function of the quantum system called quantum-classical fidelity (QCF). In the analysed regime the QCF strongly deviates from the known general behaviour discussed in Horvat *et al* (2006 *Nonlinearity* **19** 1–23 (*Preprint* quant-ph/0601139)), in particular it decays faster than exponential. Here we study and explain the observed behaviour of the QCF and the apparent violation of the QCC principle.

PACS numbers: 03.65.−w, 03.65.Yz, 05.45.Mt

1. Introduction

The quantum-classical correspondence (QCC) is the basic principle underlying any physical quantization of a classical system. According to this principle the quantum system should behave in a manner similar to that of the corresponding classical system with increasing energy or a decreasing effective Planck constant. The importance of the QCC as a tool in the study of quantum systems was recognized very early in the development of quantum mechanics with the Ehrenfest theorem and later by the introduction of semi-classical methods [2]. The study of QCC gave in the 1980s birth to quantum chaology—research area devoted to study the connections between dynamical properties of classical systems and corresponding quantum systems [3].

The QCC can be explored and discussed using various tools and methods available in the theory of classical/quantum systems. In a recent paper [1], a phase-space representation has been used to study the time evolution of QCC in generic chaotic systems on compact classical phase space.

The QCC is there quantified using the so-called quantum-classical fidelity (QCF), namely the integrated overlap between the classical phase-space density and the corresponding Wigner function. It has been shown that in classically chaotic systems, after some initial plateau, the QCF decays exponentially in time with a decay rate coinciding with the maximal Lyapunov exponent λ. While it is common knowledge in the realm of quantum chaos that the phase-space correspondence between classical and quantum mechanics drops down on the scale of Ehrenfest time $t_E \approx -\log\hbar/\lambda$, the exact dependence of initial plateau on dynamical properties and on Hilbert space dimension is still an important open question that we aim to address here, at least in a special case. In particular, here we discuss the QCC using QCF for the so-called perturbed Arnold cat map [4] on a torus $\mathbb{T}^2 = [0,1]^2$. The (unperturbed) cat map is a paradigmatic example of a classical uniformly hyperbolic chaotic systems. It has been one of the first extensively studied quantum maps [5], and since then it has been used several times to prove or disprove various conjectures concerning statistical properties of eigenfunctions for quantum system with strongly chaotic classical motion (see for example [6] and references therein). Because of the linearity of the classical motion, its quantum counterpart inherits a natural non-generic number-theoretical structure, reflected for example in the rigid distribution of eigenvalues and also in the so-called *exactness* of the Egorov property, which roughly means that classical and quantum time evolution perfectly commute. A generic behaviour of eigenvalue statistics, namely a good agreement with the predictions of random matrix theory, can be gained by perturbing the linear cat dynamics by composing it with a time one flow generated by a global Hamiltonian [7, 8].

We are here interested in exploring the time evolution properties of these perturbed maps. In particular, we aim to study how QCC decays in the presence of perturbation and especially the time scales of the initial plateau in QCF.

2. Quantization on a torus and Egorov property

We recall here the basic facts of quantum mechanics over the torus which we need in the paper; see [6, 9] for further details. The system is quantized on a torus $\mathbb{T}^2$ by introducing a position basis $\{|q_n\rangle : q_n = \frac{n}{N}\}_{n\in\mathbb{Z}_N}$ and a momentum basis $\{|p_m\rangle : p_m = \frac{m}{N}\}_{m\in\mathbb{Z}_N}$ in the Hilbert space $\mathcal{H}_N$ of dimension N. We apply periodic boundary conditions $|q_{n+N}\rangle = |q_n\rangle$ and $|p_{m+N}\rangle = |p_m\rangle$. The two bases are related to the discrete Fourier transform

$$\langle q_n|p_m\rangle = \frac{1}{\sqrt{N}}\,\mathrm{e}^{\mathrm{i}\frac{2\pi}{N}nm}. \tag{1}$$

Then according to the Weyl–Wigner quantization we associate an operator $\hat{A}$ with a classical observable a defined over grid points $\mathcal{G}_N = \{x_{n,m} = (\frac{n}{2N}, \frac{m}{2N})\}_{(n,m)\in\mathbb{Z}^2_{2N}}$ on classical phase space $\mathbb{T}^2$ using the following relations:

$$a_{n,m} = \mathrm{tr}\{\hat{A}\hat{A}_{n,m}\}, \qquad \hat{A} = \hat{Q}_{\mathrm{w}}(a) = \sum_{(n,m)\in\mathbb{Z}^2_{2N}} a_{n,m}\hat{A}_{n,m}, \tag{2}$$

where $\hat{A}_{n,m}$ is called the point operator or the kernel of the Weyl–Wigner formalism

$$\hat{A}_{n,m} = \frac{\mathrm{e}^{\mathrm{i}\frac{\pi}{N}nm}}{2\sqrt{N}} \sum_{k\in\mathbb{Z}_N} \mathrm{e}^{-\mathrm{i}\frac{2\pi}{N}km}|q_{n-k}\rangle\langle q_k|. \tag{3}$$

We say that a is the phase-space representation of the operator $\hat{A}$ or $\hat{A}$ is the quantization of the phase-space function a. The phase-space representation of a density operator corresponding to a pure state $\hat{\rho} = |\psi\rangle\langle\psi|$ is the Wigner function $W_\psi(n, m)$ defined as

$$W_\psi(n,m) = \frac{\mathrm{e}^{\frac{\mathrm{i}\pi}{N}nm}}{2\sqrt{N}} \sum_{k\in\mathbb{Z}_N} \langle\psi|q_{n-k}\rangle\langle q_k|\psi\rangle\, \mathrm{e}^{-\mathrm{i}\frac{2\pi}{N}km}, \qquad (n,m)\in\mathbb{Z}^2_{2N}, \tag{4}$$

with normalization $\sum_{(n,m)\in\mathbb{Z}^2_{2N}} W_\psi(n,m)^2 = 1$. Namely,

$$\hat{Q}_{\mathrm{w}}(W_\psi) = \hat{\rho} = |\psi\rangle\langle\psi|. \tag{5}$$

Let us assume that $M : \mathbb{T}^2 \to \mathbb{T}^2$ is a classical discrete, area preserving, map on the torus. Then it is possible to associate a corresponding quantum evolution operator $\hat{U} : \mathcal{H}_N \to \mathcal{H}_N$ with M. In the following, N is always an even integer in order to avoid certain technicalities in quantization (see [6] and references therein). The propagator $\hat{U}$ will satisfy an *Egorov estimate*, namely [10]:

$$\lim_{N\to\infty} \|\hat{U}^\dagger \hat{Q}_{\mathrm{w}}(a)\hat{U} - \hat{Q}_{\mathrm{w}}(a\circ M)\| = 0. \tag{6}$$

In particular, if the classical map is a linear automorphisms i.e. $M(\mathbf{x}) = \mathbf{M}.\mathbf{x}$, where matrix $\mathbf{M} \in SL(2,\mathbb{Z})$ (e.g. the cat map) then *Egorov is exact*:

$$\hat{U}^\dagger \hat{Q}_{\mathrm{w}}(a)\hat{U} = \hat{Q}_{\mathrm{w}}(a\circ M). \tag{7}$$

3. Cat map and breaking of Egorov property

The classical dynamics over the torus that we study here is given by the map $M : \mathbb{T}^2 \to \mathbb{T}^2$:

$$(q,p)' = M(q,p), \qquad \begin{array}{lll} p' = p + kq + \boldsymbol{\epsilon}\cdot\dot{\mathbf{V}}(q) & \mathrm{mod} & 1 \\ q' = q + p' & \mathrm{mod} & 1, \end{array} \tag{8}$$

with $k \in \mathbb{N}$, perturbation parameters $\boldsymbol{\epsilon} = (\epsilon_0, \epsilon_1, \epsilon_2) \in \mathbb{R}^3$ and perturbation function

$$\mathbf{V}(q) = \left(\frac{1}{2}q^2, -\frac{1}{2\pi}\cos(2\pi q), q\right). \tag{9}$$

The quantum evolution operator corresponding to the perturbed cat map $\hat{U}$ can be written as

$$\hat{U} = \exp\left(-\mathrm{i}\frac{\pi}{N}\hat{m}^2\right)\exp\left(\mathrm{i}k\frac{\pi}{N}\hat{n}^2 + \mathrm{i}N\boldsymbol{\epsilon}\cdot\hat{\mathbf{V}}\right), \qquad \hat{\mathbf{V}} = \mathbf{V}\left(\frac{2\pi}{N}\hat{n}\right), \tag{10}$$

where we have for convenience introduced auxiliary operators

$$\hat{n}|q_n\rangle = n|q_n\rangle, \qquad \hat{m}|p_m\rangle = m|p_m\rangle. \tag{11}$$

If the perturbations are neglected $\boldsymbol{\epsilon} = 0$, we obtain the usual linear cat map system, where the map and evolution operator are denoted by

$$M_{\mathrm{c}} = M|_{\epsilon=0}, \qquad \hat{U}_{\mathrm{c}} = \hat{U}|_{\epsilon=0}. \tag{12}$$

As already remarked, it is well known that this system is Egorov exact. Moreover, the classical cat map is uniformly hyperbolic with the Lyapunov exponent

$$\lambda(k) = \log\left[\tfrac{1}{2}(k+2+\sqrt{k(k+4)})\right]. \tag{13}$$

For the coming analysis, it is convenient to write the classical map and the quantum evolution operators of the perturbed cat map as

$$\hat{U} = \hat{U}_{\mathrm{c}}\exp\left(\mathrm{i}N\boldsymbol{\epsilon}\cdot\hat{\mathbf{V}}\right), \qquad M = M_{\mathrm{c}} + (\boldsymbol{\epsilon}\cdot\dot{\mathbf{V}}, \boldsymbol{\epsilon}\cdot\dot{\mathbf{V}}). \tag{14}$$

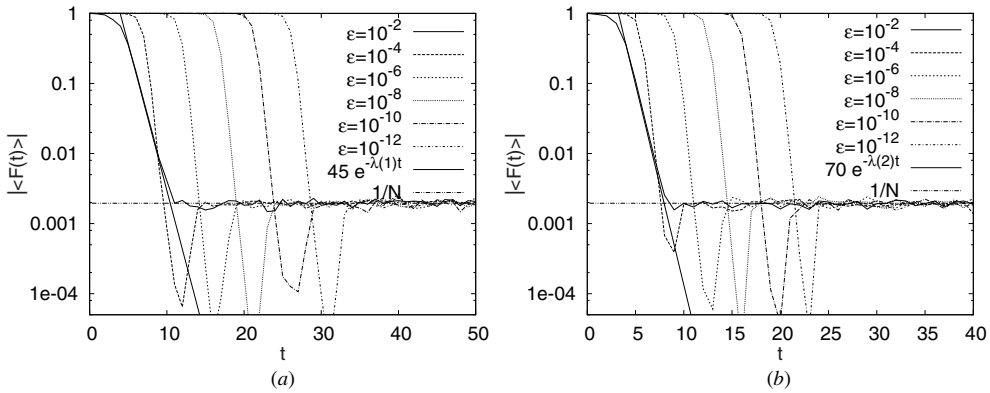

Figure 1. The average QCF $F(t)$ with perturbation vector $\epsilon = (\epsilon, 0, 0)$ for different perturbations strength ϵ at Hilbert space dimension $N = 512$ and $k = 1, 2$ (a), (b). The average is taken over 100 initial Gaussian packets uniformly scattered over phase space.

We compare the classical and quantum evolution of the perturbed cat map in the classical phase space at some fixed dimension N and perturbation ϵ. The $\epsilon = \|\epsilon\|$ is refereed to as the perturbation strength. Here we are mainly interested in the particular case of semiclassical small perturbations $N\epsilon \ll 1$. More precisely, the classical system starts from a smooth probability distribution $\rho : \mathbb{T}^2 \to \mathbb{R}$ resembling a Gaussian packet on phase space at the point (q_0, p_0),

$$\rho_{(q_0,p_0)}(q, p) = D_{N,(q_0,p_0)} \left(\sum_{\nu\in\mathbb{Z}} \mathrm{e}^{-2\pi N(q-q_0+\nu)^2} \right) \left(\sum_{\nu\in\mathbb{Z}} \mathrm{e}^{-2\pi N(p-p_0+\nu)^2} \right), \quad (15)$$

where the scalar factor D_N is pinned down by the normalization

$$\sum_{(n,m)\in\mathbb{Z}^2_{2N}} \rho^2_{(q_0,p_0)}(x_{n,m}) = 1, \quad (16)$$

which has a simple leading term in the asymptotic approximation, $N \to \infty$, reading

$$D_{N,(q_0,p_0)} \asymp \frac{1}{\sqrt{N}} [(1 + 2\cos(4\pi N q_0)\,\mathrm{e}^{-\pi N})(1 + 2\cos(4\pi N p_0)\,\mathrm{e}^{-\pi N})]^{-\frac{1}{2}}. \quad (17)$$

The quantum counterpart is initially in a coherent state $|\phi\rangle$ with a Wigner function W_ψ similar to the classical distribution (see [1, 11]):

$$W_\phi(n, m) = \rho(x_{n,m}) + \mathrm{e}^{-|O(N)|}, \qquad (n, m) \in \mathbb{Z}^2_{2N}. \quad (18)$$

We then let these two systems evolve up to time $t \in \mathbb{Z}^*$ using equations

$$\rho^t = \rho \circ M^{-t}, \qquad |\phi^t\rangle = \hat{U}^t|\phi\rangle, \qquad \hat{\rho}^t = \hat{U}^t \hat{\rho} \hat{U}^{-t}, \quad (19)$$

and observe the QCC between these two systems by calculating the overlap of the density ρ^t and corresponding Wigner function W_{ϕ^t}. The overlap is called quantum-classical fidelity (QCF) defined as

$$F(t) = \sum_{(n,m)\in\mathbb{Z}^2_{2N}} W_{\psi^t}(n, m)\rho^t(x_{n,m}) = \mathrm{tr}\{\hat{\rho}^t \hat{Q}(\rho^t)\} \leqslant 1 + \mathrm{e}^{-|O(N)|}. \quad (20)$$

Because the perturbed system is not Egorov exact, the QCF decreases with time. In figure 1 we show the decay of an average QCF $\langle F(t)\rangle$ for different k and perturbation strengths ϵ using

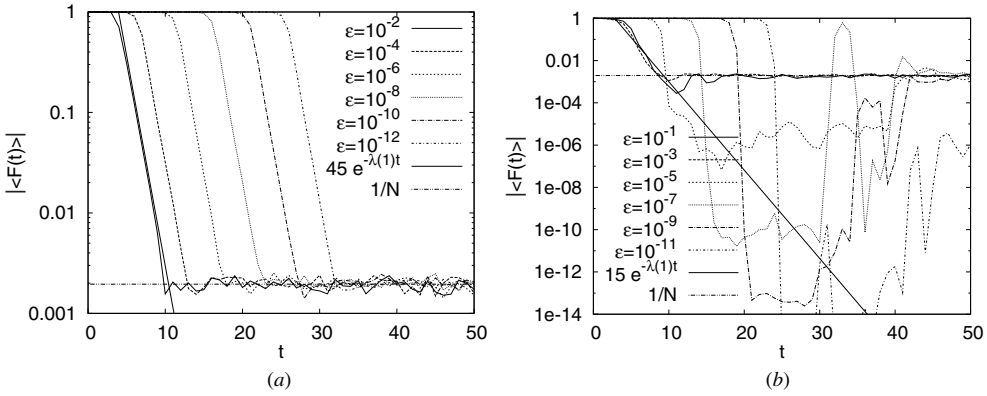

Figure 2. The average QCF $F(t)$ for different perturbation strengths ϵ with perturbation vector $\epsilon = (0, \epsilon, 0)$, $(0, 0, \epsilon)$ (a), (b) at Hilbert space dimension $N = 512$ and $k = 1$. For averaging see caption of figure 1.

the perturbation vector $\boldsymbol{\epsilon} = (\epsilon, 0, 0)$, where $\langle\bullet\rangle$ denotes the uniform average taken over the initial positions of the coherent packet. The QCF does not decay up to time called the breaking time t_{br}, which increases with decreasing perturbation. Beyond t_{br} the QCF decays 'very fast' (as we will argue, faster then exponential) and eventually converges to the ergodic plateau given by $1/N$: the decay is in fact visually faster than the generally expected exponential Lyapunov decay $\langle F(t)\rangle \sim \exp(-\lambda t)$ [1], which is shown in the figures. Basically, the same scenario occurs in other choices of perturbation vectors $\boldsymbol{\epsilon}$ as we can see in figure 2. In the case of constant classical perturbation $\boldsymbol{\epsilon} = (0, 0, \epsilon)$ shown in figure 2(b), the correspondence is broken mainly by a rigid shifting of the deformed packets in the quantum and classical picture. Therefore the convergence towards the ergodic plateau is less smooth as in other cases. At this point it is difficult to deduce the correct functional form of the QCF $F(t)$. Nevertheless, in the following we present a theoretical explanation of these numerical observations, disclosing the super-exponential nature of the QCF decay in this particular regime of. perturbation.

We are interested in the evolution of the QCF in the limit of small perturbations $\epsilon \to 0$. In this regime we examine the time $t_{\mathrm{br}}(p)$ on which an average QCF $\langle F(t)\rangle$ drops below some value p:

$$t_{\mathrm{br}}(p) = \min\{t \in \mathbb{Z}^* : \langle F(t)\rangle < p\}, \tag{21}$$

where the average $\langle\bullet\rangle$ is taken uniformly over positions of the initial Gaussian packets. It is meaningful to express the dynamics relative to the unperturbed cat map writing

$$\rho^t = \rho_{\mathrm{c}}^t + \delta\rho^t, \qquad \hat{\rho}^t = \hat{\rho}_{\mathrm{c}}^t + \delta\hat{\rho}^t, \tag{22}$$

where the dynamics of the cat map case is given by

$$\hat{\rho}_{\mathrm{c}}^t = \hat{U}_{\mathrm{c}}^t \hat{\rho} \hat{U}_{\mathrm{c}}^{-t}, \qquad \rho_{\mathrm{c}}^t = \rho \circ M_{\mathrm{c}}^{-t}. \tag{23}$$

and due to the Egorov property these are connected by

$$\hat{\rho}_{\mathrm{c}}^t = \hat{Q}\big(\rho_{\mathrm{c}}^t\big). \tag{24}$$

By inserting ansätz (22) into formula (20) we obtain the QCF expressed in terms of deviations from the unperturbed case

$$F(t) = 1 + \mathrm{tr}\big\{\delta\hat{\rho}^t \hat{Q}\big(\rho_{\mathrm{c}}^t\big)\big\} + \mathrm{tr}\big\{\hat{\rho}_{\mathrm{c}}^t \hat{Q}(\delta\rho^t)\big\} + \mathrm{tr}\{\delta\hat{\rho}^t \hat{Q}(\delta\rho^t)\}. \tag{25}$$

Due to the existence of the Egorov property in the cat map, the approximated QCF can be expressed in terms of the quantum fidelity $F_q(t)$ [12] and the classical fidelity $F_c(t)$ [13] as

$$F(t) = |F_q(t)|^2 + F_c(t) - 1 + \mathrm{tr}\{\delta\hat{\rho}^t\,\hat{Q}(\delta\rho^t)\}, \tag{26}$$

where F_q and F_c are written as

$$F_q(t) = \langle\phi|\hat{U}^{-t}\hat{U}_c^t|\phi\rangle, \qquad F_c(t) = \sum_{(n,m)\in\mathbb{Z}_{2N}^2} \rho(M^{-t}(x_{n,m}))\rho\big(M_c^{-t}(x_{n,m})\big). \tag{27}$$

Relation (26) is very instructive and helps to understand the behaviour around the initial plateau, but it seems to us that the study of the plateau itself was greatly avoided in the past. In the following we discuss the second and the third terms in (25) denoted by

$$I_1 = \mathrm{tr}\big\{\hat{\rho}_c^t\,\hat{Q}(\delta\rho^t)\big\} = \sum_{(n,m)\in\mathbb{Z}_{2N}^2} \rho_c^t(x_{n,m})\delta\rho^t(x_{n,m}), \tag{28}$$

$$I_2 = \mathrm{tr}\big\{\delta\hat{\rho}^t\,\hat{Q}\big(\rho_c^t\big)\big\} = \mathrm{tr}\big\{\delta\hat{\rho}^t\,\hat{\rho}_c^t\big\}. \tag{29}$$

The last terms in (25) and (26) are the second-order corrections, which we do not discuss in detail. In order to understand I_1 (28) we discuss the deviation between trajectories of a chaotic and ergodic map $\phi = M^{-1} : \mathbb{T}^2 \to \mathbb{T}^2$ and of its perturbation $\phi + \delta\phi = (M + \delta M)^{-1}$, starting at the same point x. The deviation is defined as

$$\delta\phi_t(x) := (\phi + \delta\phi)^t(x) - \phi^t(x), \qquad \phi^{t+1}(x) = \phi^t(\phi(x)) \tag{30}$$

and obeys in the limit $\delta\phi \to 0$ the following recursion:

$$\delta\phi_{t+1}(x) = (\phi + \delta\phi)(\phi^t(x) + \delta\phi_t(x)) - \phi^{t+1}(x), \tag{31}$$

$$\doteq (\nabla\phi)(\phi^t(x))\delta\phi_t(x) + \delta\phi(\phi^t(x)), \tag{32}$$

where we have neglected second-order corrections. By iterating this equations from a given initial position x, the deviation is written as a series

$$\delta\phi_t(x) = \sum_{k=0}^{t-1}\left[\prod_{l=k}^{t-1}(\nabla\phi)(\phi^l(x))\right]\delta\phi(\phi^{k-1}(x)) + \delta\phi(\phi^{t-1}(x)). \tag{33}$$

By taking into account that map is chaotic and ergodic with the Lyapunov exponent λ, we get in the limits $t \to \infty$ and $\delta\phi \to 0$, applied in given order, the leading contribution of the deviation expressed as

$$\delta\phi_t(x) = O(\delta\phi)\,\mathrm{e}^{\lambda t}, \qquad \langle\|\delta\phi_t(x)\|\rangle \approx \epsilon A\,\mathrm{e}^{\lambda t}, \tag{34}$$

where $\langle\bullet\rangle$ denotes the uniform average over initial positions x. The constant $A \in \mathbb{R}$ depends only on the type of perturbation and dynamical properties of the map. By plugging this result into expression I_1 (28) we obtain

$$I_1 = \sum_{(n,m)\in\mathbb{Z}_{2N}^2} \rho(x_{n,m})\rho(x_{n,m} + \delta\tilde{\phi}_t(x_{n,m})) - 1, \qquad \delta\tilde{\phi}_t = \delta\phi_t \circ M^t, \tag{35}$$

where we have used that the cat map M conserves the grid G_N: $M(G_N) = G_N$. Then by taking into account the explicit form of ρ (15) and considering only the behaviour about the central point of the Gaussian packet the above expression is approximated as

$$I_1 \approx \exp(-\pi N\|\delta\tilde{\phi}_t(q_0, p_0)\|^2) - 1, \qquad \langle I_1\rangle \approx \exp(-\pi N A^2\epsilon^2\exp(2\lambda t)), \tag{36}$$

with $\langle\bullet\rangle$ representing the uniform average over position of the initial coherent packet. The approximation is meaningful up to times $\epsilon N^{\frac{1}{2}}\exp(\lambda t) = O(1)$, when deformation of the

packets can be neglected. This is especially appropriate to describe the case of constant classical perturbation. In the limit of small perturbations the leading term in expression I_1 scales with time and perturbation as $O(N\epsilon^2 \exp(2\lambda t))$, where the changes of QCF are small. The behaviour of the expression I_1 is obtained by considering the fact that

$$\hat{U}^t = \hat{U}_c^t + \mathrm{i}N\boldsymbol{\epsilon} \cdot \sum_{k=1}^{t} \hat{U}_c^k \hat{\mathbf{V}} \hat{U}_c^{t-k} + O((N\|\boldsymbol{\epsilon}\hat{\mathbf{V}}\|)^2 t), \tag{37}$$

which yields

$$\delta\hat{\rho}^t = \mathrm{i}N\boldsymbol{\epsilon} \cdot \left[\hat{\mathbf{S}}^t \hat{\rho}_c^t - \hat{\rho}_c^{-t} \hat{\mathbf{S}}^{-t}\right] + O((N\|\boldsymbol{\epsilon}\hat{\mathbf{V}}\|)^2 t), \tag{38}$$

$$\hat{\mathbf{S}}^t = \sum_{k=1}^{t} \hat{U}_c^{-k} \hat{\mathbf{V}} \hat{U}_c^k. \tag{39}$$

By plugging this into I_2 (29) we get

$$I_2 = 2N\boldsymbol{\epsilon} \cdot \Im\left\{\mathrm{tr}\left\{\hat{\mathbf{S}}^t \hat{\rho}_c^t\right\}\right\} + O((N\|\boldsymbol{\epsilon}\hat{\mathbf{V}}\|)^2 t). \tag{40}$$

By assuming that $\lim_{t\to\infty} t^{-1}\hat{\mathbf{S}}^t \neq 0$ we see that the leading term in I_2 scales as $O(N\epsilon t)$ in time. Then by considering results I_1 (36) and I_2 (40) we get the leading-order contributions to the QCF reading

$$F(t) \approx 2N\boldsymbol{\epsilon} \cdot \Im\left\{\mathrm{tr}\left\{\hat{\mathbf{S}}^t \hat{\rho}_c^t\right\}\right\} + \exp(-\pi N\|\delta\tilde{\phi}_t(q_0, p_0)\|^2). \tag{41}$$

In the limit of the small perturbations the last term in (41) is dominant. This is also supported numerically as shown in figure 3, where we show $G(t) = \log(-\log(\langle F(t)\rangle))$ for different perturbation vectors $\boldsymbol{\epsilon}$, perturbation strength ϵ and k. We see that the average QCF evolves following the curve $G(t) \approx 2\lambda(k)t + \mathrm{const}$ according to the dominant term in QCF $I_1(t)$ (36) almost up to the time, when QCF intersects the ergodic plateau given by $G(t) \approx \log\log N$. The plot $G(t)$ has an initial plateau due to finite arithmetic. We conclude that the QCF decays in average towards the ergodic plateau faster than exponentially as

$$\langle F(t)\rangle = \exp(-|O(\exp(|O(t)|))|). \tag{42}$$

The expression for QCF (41) obtains in the limit $\sqrt{N}\epsilon \exp(\lambda t) \ll 1$ a simple scaling form

$$\langle F(t)\rangle = 1 - O(N\epsilon^2 \mathrm{e}^{2\lambda t}) + O(N\epsilon t), \tag{43}$$

where the first non-constant term is dominant in $F(t)$. In this perturbation approach we can approximate $t_{\mathrm{br}}(p)$ (21) for fixed $1 - p \ll 1$ as

$$t \approx \frac{\log(1-p) - \log(N\epsilon^2)}{2\lambda}, \tag{44}$$

which in the limit of infinitesimal perturbations obtains the following asymptotic form:

$$\lambda t_{\mathrm{br}} \asymp -\log\epsilon, \qquad \epsilon \to 0. \tag{45}$$

We see that at fixed N and p the time depends only on the Lyapunov exponent λ and perturbation strength ϵ.

4. Numerical result on the breaking time

In the following we present numerical results of the breaking time t_{br} in our perturbed cat map. We explore in particular its dependence on the perturbation strength ϵ and the Hilbert space dimension N.

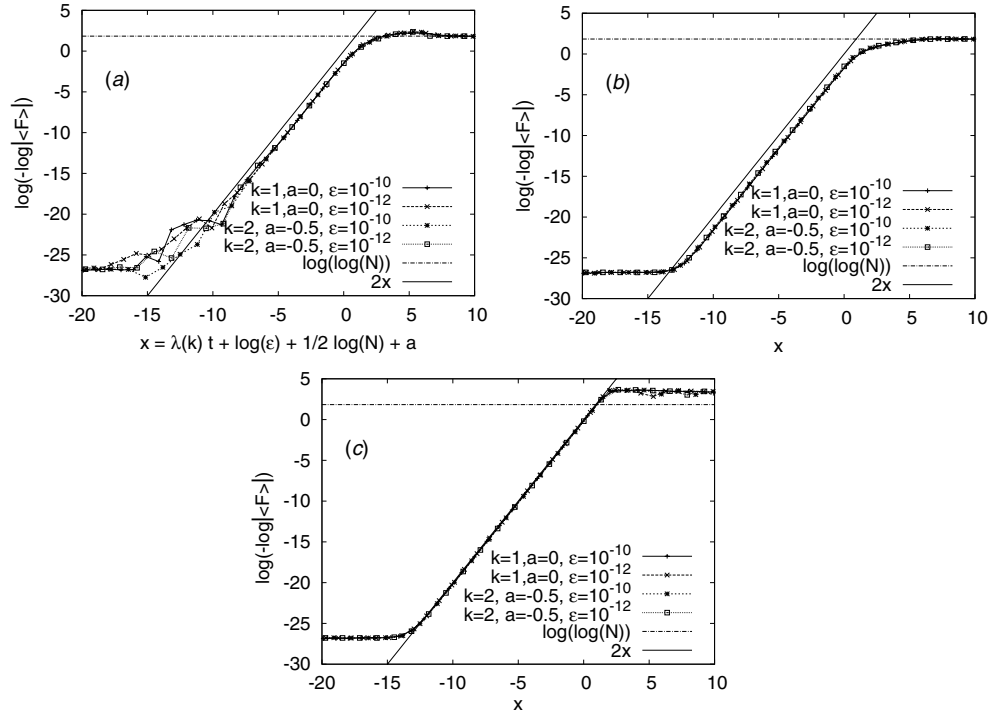

Figure 3. The representation of average QCF $\langle F(t)\rangle$ evolution calculated using perturbation vector ϵ equal to $(\epsilon, 0, 0)$ (a), $(0, \epsilon, 0)$ (b) and $(0, 0, \epsilon)$ (c) for different ϵ and $k = 1, 2$ at the dimension $N = 512$, where data presented in figures 1 and 2 are also considered. For averaging see the caption of figure 1.

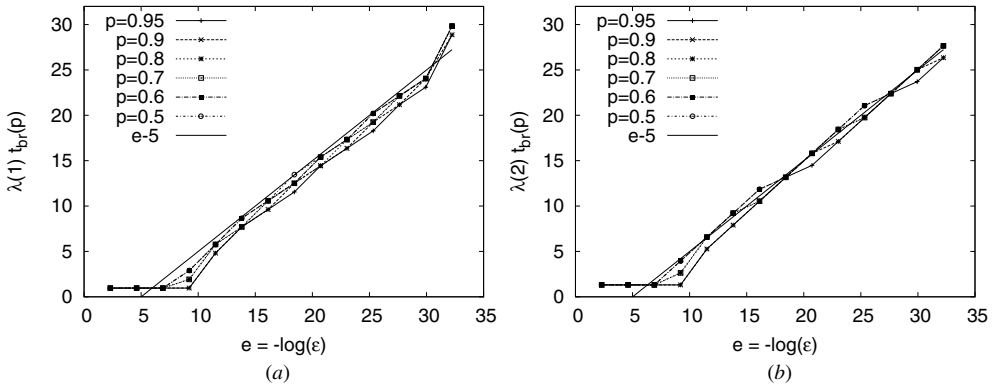

Figure 4. The dependence of $t_{\rm br}$ on perturbation strength ϵ in the cases $k = 1$ (a) and $k = 2$ (b) by using perturbation vector $\epsilon = (\epsilon, 0, 0)$ at $N = 512$.

Figures 4 and 5 show the plots of $t_{\rm br}$ in dependence of ϵ for all three types of the perturbations. Because we are discussing a discrete dynamical system, the break time $t_{\rm br}(\epsilon, p)$ is a discrete function of $\epsilon \in \mathbb{R}^+$. In figure 4 we show $t_{\rm br}$ as a function of ϵ in

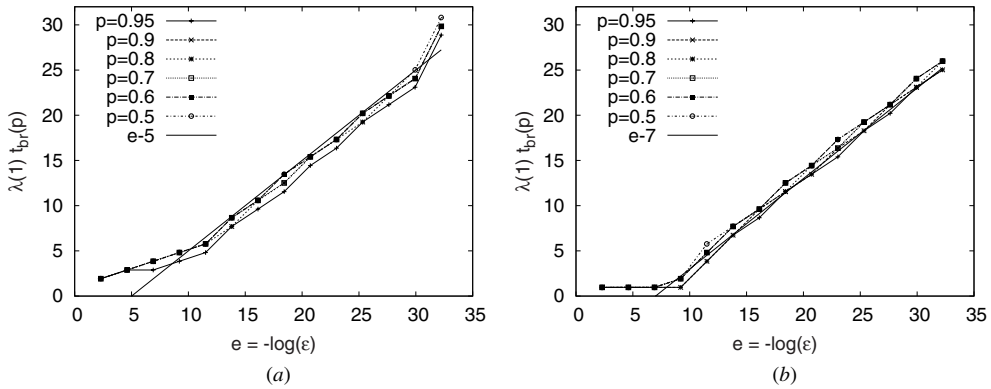

Figure 5. The dependence of $t_{\rm br}$ on perturbation strength ϵ in the case of perturbation vectors $\epsilon = (0, \epsilon, 0), (0, 0, \epsilon)$ (a), (b) at $N = 512$ and $k = 1$.

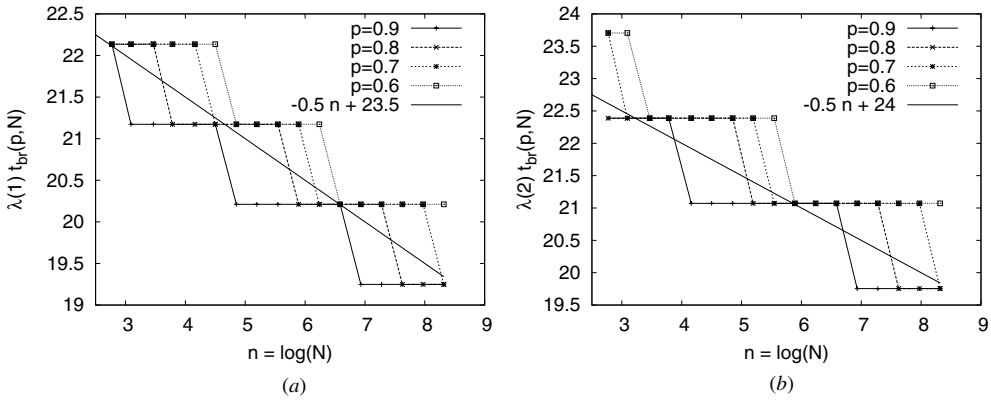

Figure 6. The dependence of $t_{\rm br}$ of Hilbert space dimension N at perturbation $\epsilon = (10^{-10}, 0, 0)$ in the case $k = 1$ (a) and $k = 2$ (b).

the case of non-smooth perturbation $\epsilon = (\epsilon, 0, 0)$ for two values of the classical parameter k. In order to improve representation we show plots for several p at the same time. We see that the heuristically obtain formula $\lambda t_{\rm br} \sim -\log \epsilon$ fit perfectly onto the numerical results. The dependence of $t_{\rm br}$ on ϵ in the presence of smooth perturbations is shown in figure 5. We note that the gross dependence of the break time is basically independent of perturbation.

The break time $t_{\rm br}$ (21) also depends on the Hilbert space dimension N. In the limit of small perturbations $\epsilon N \ll 1$ we obtain from (44) the following dependence on N:

$$\lambda t_{\rm br} \approx \text{const} - \tfrac{1}{2} \log N, \tag{46}$$

where the constant depends on p, λ and details of the initial packets. The numerical results shown in figures 6 and 7 in the case of using smooth and non-smooth perturbation, respectively, confirm the theoretical dependence. But due to insufficient range in variable $\log N$ we cannot check the prefactor in scaling relation (46) very accurately.

Note that the break time $t_{\rm br}$ is decreasing with increasing N. At the first look this would appear as a contradiction to the known QCC principle, which states that the quantum system

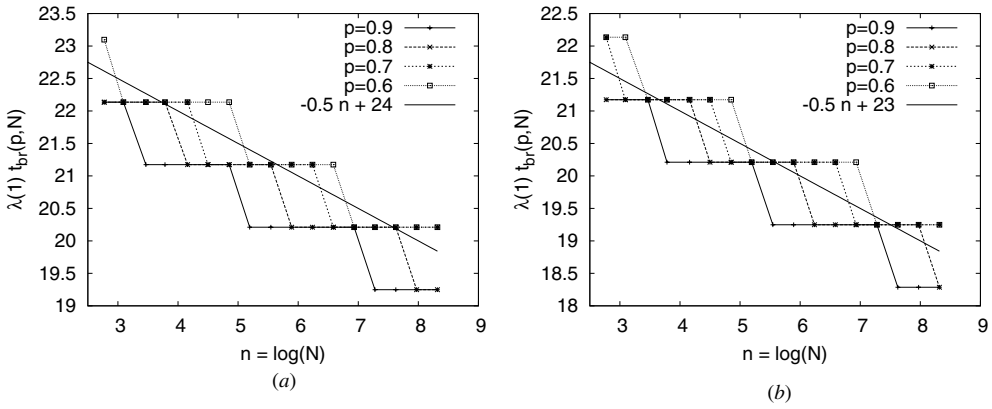

Figure 7. The dependence of t_{br} of Hilbert space dimension N at perturbation vectors $\epsilon = (0, 10^{-10}, 0), (0, 0, 10^{-10})$ (a, b) for $k = 1$.

should behave as the classical system in the limit $N \to \infty$. But this is not the case: with increasing N eventually $N\epsilon \sim 1$ and the perturbation approach becomes invalid. Thereby we enter the general regime discussed in [1], where the break time t_{br} scales with N as

$$\lambda t_{\mathrm{br}} \asymp C \log N, \tag{47}$$

where constant C depends on the type of perturbation. Therefore everything is still consistent with the QCC principle.

5. Conclusions

In this paper we investigate the correspondence between the classical and quantum dynamics of the perturbed cat map on the torus in the limit of semiclassical small perturbations. The correspondence is measured by the overlap between the classical density and the Wigner function called quantum-classical fidelity (QCF) and denoted by $F(t)$. We study the time evolution of QCF, which stays for a long time at the initial value $F(t) \approx 1$ and then decays towards the ergodic value $F(t) \approx 1/N$ faster than generally expected. The length of the initial plateau t_{br} scales with perturbation ϵ and Hilbert space dimension as $\lambda t_{\mathrm{br}} \sim -\log(N^{\frac{1}{2}}\epsilon)$, where λ is the maximal Lyapunov exponent. At the first moment the scaling with N seems to be in contradiction with the correspondence principle, but this is not the case because the result is only meaningful for $\epsilon N \ll 1$. In this particular perturbation regime, the observed behaviour is clearly far from general and hence the results presented here for the important and historical model of the (perturbed) cat map supplement the general knowledge of the QCC in evolving chaotic systems discussed in [1]. It is important to note that the presented results can be applied to arbitrary chaotic systems which are *almost Egorov exact* or such that the Egorov exactness can be broken by a weak perturbation.

Acknowledgments

MH would like to thank Dipartimento di Matematica in Bologna, Italy, and Ministry of Higher Education, Science and Technology of Slovenia for their financial support.

References

[1] Horvat M, Prosen T and Degli Esposti M 2006 Quantum-classical correspondence on compact phase space *Nonlinearity* **19** 1–23 (*Preprint* quant-ph/0601139)

[2] Landau L D and Lifschitz E M 1991 *Quantum Mechanics, Non-relativistic Theory* 3rd edn (Oxford: Pergamon)

[3] Haake F 2001 *Quantum Signatures of Chaos* 2nd edn (Heidelberg: Springer)

[4] Arnold V I and Avez A 1989 *Ergodic Problems of Classical Mechanics* (Reading, MA: Addison-Wesley)

[5] Hannay J H and Berry M V 1980 Quantization of linear maps on the torus—Fresnel diffraction by a periodic grating *Physica* D **1** 267–90

[6] Degli Esposti M and Graffi S 2003 *The Mathematical Aspects of Quantum Maps (Lecture Notes in Physics* vol 618*)* (Berlin: Springer)

[7] de Matos M B and de Almeida A M O 1995 Quantization of Anosov map *Ann. Phys., NY* **237** 46–65

[8] Boasman P A and Keating J P 1995 Semiclassical asymptotics of perturbed cat maps *Proc. R. Soc. Lond.* A **449** 629–53

[9] Dana I 2002 General quantization of canonical maps on a two-torus *J. Phys. A: Math. Gen.* **35** 3447–65

[10] De Bièvre S and Degli Esposti M 1998 Egorov theorems and equidistribution of eigenfunctions for the quantized sawtooth and Baker maps *Ann. Inst. Henri Poincare Phys. Theor.* **69** 1–30

[11] Nonnenmacher S 2006 On evolution and scarring for perturbed quantum cat maps (Private communication)

[12] Gorin T, Prosen T, Seligman T H and Žnidarič M 2006 Dynamics of loschmidt echoes and fidelity decay *Phys. Rep.* **435** 33–156

[13] Veble G and Prosen T 2004 Faster than Lyapunov decays of classical Loschmidt echo *Phys. Rev. Lett.* **92** 34101